Modelling of the recirculation in mechanical-draught heat exchangers

C. G. du Toit* and D. G. Kröger**
(First and final version March 1992)

Abstract

The two-dimensional air flow pattern about a forced-draught heat exchanger is modelled numerically and investigated analytically. A thorough understanding of the flow field and associated phenomena is imperative for the optimal design of such systems.

The governing equations are discretized using the finite volume method. The general purpose fluid-flow code PHOENICS is used to model the flow field. The turbulent nature of the flow is modelled using the standard k-ε turbulence model as incorporated in PHOENICS.

The influence of recirculating warm plume air on the performance of mechanical-draught heat exchangers is investigated and compared with analytical, experimental and other numerical data.

The numerical results compare favourably with the analytical and experimental data, as well as with the expected general flow pattern.

Nomenclature

A	area
C_1, C_2, C_μ	constants in turbulence equations
c_p	specific heat
e	effectiveness
G	production term
g	gravitational acceleration
H	height
k	turbulent kinetic energy
$\dot{m}$	mass flow rate
Pr	Prandtl number
p	pressure
R	gas constant
r	recirculation factor
S_ϕ	source term
T	temperature
U	overall heat transfer coefficient
u	horizontal velocity component
v	vertical velocity component
V	velocity
W	width
x	horizontal coordinate
y	vertical coordinate
δt_f	false time step
Γ_ϕ	diffusion coefficient
ε	dissipation rate of turbulent kinetic energy
μ	dynamic viscosity
ρ	density
σ_k	"Prandtl number" for k
σ_ε	"Prandtl number" for ε
ϕ	general variable
ω	linear relaxation parameter

Subscripts

a	ambient
e	effective
he	heat exchanger condition
i	inlet condition
o	outlet condition
r	recirculation
ref	reference value
t	turbulent
w	wall

Introduction

A cross-section of one half of a two-dimensional mechanical-draught heat exchanger and the associated air flow pattern is depicted in Figure 1. In the absence of wind, the buoyant plume or jet rises vertically above the heat exchanger. This results in ambient air being drawn in underneath the heat exchanger and sets up a large recirculating cell. Some of the ambient air is also dragged along by the

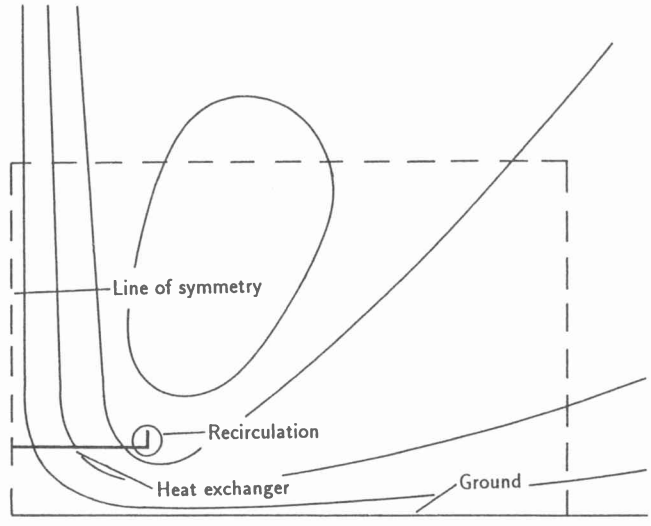

Fig. 1 Qualitative flow pattern

* Chief Researcher
** Professor in Mechanical Engineering (Member)
Department of Mechanical Engineering, University of Stellenbosch, 7600 Stellenbosch

rising plume and this also acts as a further driving mechanism for the cell. Part of the warm plume air may, however, be drawn back into the inlet of the heat exchanger. This phenomenon is known as "recirculation" and is confined to the area surrounding the end of the heat exchanger as opposed to the larger scale circulation mentioned above. This phenomenon can have an adverse influence on the performance of the heat exchanger and therefore indirectly reduces its effective size.

The results of numerous studies on recirculation are reported in the literature. However, most are experimental investigations performed on heat exchangers having specific geometries and operating under particular conditions, for example [1,2]. Gunter et al [3] present the results of field tests performed on air-cooled heat exchangers and define certain recirculation flow limits.

Becker et al [4] model the wind induced plume recirculation back into the intake louvres of a mechanical draught cooling tower numerically. The wind field is modelled using a stream function vorticity formulation, whilst the flow field within the tower is modelled as a porous media flow. The interior and exterior flow fields are coupled by matching pressures and flow rates at the intake louvres. The model yields results which are in good agreement with physical intuition and compare well with both basic theory and with reported laboratory and field results.

The results of an analytical, numerical and experimental investigation are reported by Kröger [5]. It is shown that the amount of recirculation that occurs is a function of the flow and the thermal and geometric characteristics of the heat exchanger. The boundary conditions which are applied in the numerical study are dealt with at length by Schreüder et al [6] and Schreüder and Du Plessis [7]. Although the results of the three approaches differ, general trends can be observed. Kröger concludes that the analytical model can be employed to predict the approximate performance effectiveness of practical mechanical-draught heat exchangers where plume air recirculation occurs.

The current study is essentially a continuation of the investigation by Kröger [5]. An improved analytical solution is presented. In the numerical analysis slightly different boundary conditions are applied at the atmospheric boundaries and the general-purpose code PHOENICS [8] is employed to provide the numerical solutions to the governing differential equations.

Governing equations

It has been shown by Spalding [9] that the time-averaged equations for the conservation of mass, momentum, temperature T, turbulence kinetic energy k and turbulence dissipation rate ε, which describe incompressible steady flow may be written in a general form. The governing equation for the general variable ϕ can be written in terms of a 2-D orthogonal coordinate system as:

$$\frac{\partial}{\partial x}(\rho u\phi)+\frac{\partial}{\partial y}(\rho v\phi)-\frac{\partial}{\partial x}\left(\Gamma_\phi\frac{\partial\phi}{\partial x}\right)-\frac{\partial}{\partial y}\left(\Gamma_\phi\frac{\partial\phi}{\partial y}\right)=S_\phi \qquad (1)$$

where $v = 1,u,v,T,k$ and ε; Γ_ϕ is the effective diffusion coefficient; S_ϕ the source term, and u and v are the velocity components in the x and y directions respectively.

ϕ	S_ϕ	Γ_ϕ
1	0	0
u	$-\frac{\partial p}{\partial x}+\frac{\partial}{\partial x}\left(\mu_e\frac{\partial u}{\partial x}\right)+\frac{\partial}{\partial y}\left(\mu_e\frac{\partial v}{\partial x}\right)$	μ_e
v	$-\frac{\partial p}{\partial y}+(\rho-\rho_{ref})g-\frac{\partial}{\partial x}\left(\mu_e\frac{\partial u}{\partial y}\right)+\frac{\partial}{\partial y}\left(\mu_e\frac{\partial v}{\partial y}\right)$	μ_e
T	$\frac{1}{c_p}\left(u\frac{\partial p}{\partial x}+v\frac{\partial p}{\partial y}+G\right)$	$\frac{\mu_e}{Pr}$
k	$G-\rho\varepsilon$	$\frac{\mu_e}{\sigma_\kappa}$
ε	$\frac{\varepsilon}{k}(C_1G-C_2\rho\varepsilon)$	$\frac{\mu_e}{\sigma_\varepsilon}$

Table 1: The form of S_ϕ and Γ_ϕ in the general equation for ϕ

The expressions for S_ϕ and Γ_ϕ in equation (1) are given in Table 1.

With the reference density ρ_{ref} set to the ambient density ρ_a, the form of the gravitational term in the v-momentum equation gives the buoyancy force that arises from differential variations of the density field about this value. This has the effect of implicitly removing the hydrostatic variation of the pressure from the pressure field. What remains in the pressure field expresses the velocity-head variations. The absence of the hydrostatic component in the pressure field also simplifies the specification of the pressure boundary conditions, for often the so-called "reduced pressure" is constant at boundaries (See Radosavljevic et al [10]).

The production term G in the equations for temperature, turbulence kinetic energy and turbulence dissipation rate is defined as follows:

$$G=\mu_e\left\{2\left[\left(\frac{\partial u}{\partial x}\right)^2+\left(\frac{\partial v}{\partial y}\right)^2\right]+\left(\frac{\partial v}{\partial x}+\frac{\partial u}{\partial y}\right)^2\right\} \qquad (2)$$

In the case of the temperature equation the source terms are assumed to be much smaller than the other terms and are therefore neglected in the simulation.

The effective viscosity μ_e is given by:

$$\mu_e=\mu+\mu_t \qquad (3)$$

where μ is the laminar dynamic viscosity of the air and μ_t the turbulent eddy viscosity. The turbulent eddy viscosity μ_t is expressed as

$$\mu_t=C_\mu'\rho\frac{k^2}{\varepsilon} \qquad (4)$$

The Prandtl number in the temperature equation is taken as $Pr = 0.71$, whilst the laminar dynamic viscosity is taken as $\mu = 1.8 \times 10^{-5}\ N \cdot s/m^2$. The empirical constants which appear in the turbulence equations are assigned the values shown in Table 2 which, according to Rodi [11], had been found to give good agreement over a wide range of two-dimensional flows.

Although the flow is assumed to be incompressible, the local density is nevertheless calculated from the ideal gas law as

$$\rho = \frac{p_a}{RT} \tag{5}$$

where $p_a = 1.013 \times 10^5\ Pa$ and the gas constant is taken as $R = 287.1\ m^2/(s^2 \cdot K)$.

C_μ	C_1	C_2	σ_k	σ_ε
0,09	1,44	1,92	1,0	1,3

Table 2: Values of Constants in Turbulence Equations

Numerical solutions

Solution Procedure

The general-purpose code PHOENICS for simulating fluid-flow, heat-transfer and chemical-reaction processes is used to solve the governing differential and associated algebraic equations. A complete description of the code PHOENICS is given by Rosten et al [12,13,14]. The governing equations are discretized using the finite volume method. In this method the computational domain is subdivided into a topologically regular grid of cells bounded by continuous lines. In order to obtain the required grid spacing at various positions in the flow field, a body-fitted non-orthogonal coordinate system is used. This also has the added advantage that various heat exchanger configurations can be modelled with relative ease. PHOENICS employs a staggered grid formulation. This means that the pressure p, the temperature T, and the turbulence kinetic energy and dissipation rate k and ε, are solved for at the cell centres. The velocity components u and v are solved for at the cell faces.

The convection terms are discretized using the hybrid upwind differencing scheme as outlined by Patankar [15]. Equations for the values of each dependent variable in each grid cell are obtained in a linearized form by the integration of the differential equations over the cells with suitable interpolation assumptions. The equations are then solved implicitly in an iterative manner. In PHOENICS the SIMPLEST pressure correction algorithm as outlined by Spalding [9] is used.

The standard k-ε turbulence model of Launder et al [16] as incorporated in PHOENICS is used to model the turbulent nature of the flow.

Computational Aspects

The non-orthogonal grid consists of 120 × 110 cells in the x- and y-directions respectively. The grid is non-uniformly spaced so as to have a greater concentration of cells where the gradients are large and where more detailed information is required. This is essentially in the vicinity of the heat exchanger and the buoyant plume.

The momentum, temperature, and k and ε equations are underrelaxed using false step relaxation, whilst the pressure, as well as the algebraically calculated values of the density and turbulent eddy viscosity are linearly underrelaxed between successive iterations. To obtain convergence each calculation normally has to be carried out in three stages, each corresponding to a different set of relaxation parameters. Typical values for the false time step and linear relaxation parameters δt_f and ω, as well as the associated number of iterations, are shown in Table 3.

Stage	δt_f			ω	Iterations
	u, v	T	k, ε		
1	1,000	10,00	0,100	0,3	≤ 50
2	0,100	1,000	0,010	0,3	100
3	0,010	0,100	0,001	0,3	≥ 300

Table 3: Typical values for the relaxation parameters

It seems as if the first stage serves the purpose of pointing the computational process in the right direction. This is then consolidated in the second stage and the solution is then refined during the last stage. The procedure can be likened to a multigrid solution where the course components are sorted out during the first stage and the finest components during the final stage.

In this analysis the atmosphere is considered to be an infinitely large mass of air of homogeneous composition in a uniform gravitational field. The boundary conditions applied in the calculation are shown in Figure 2. These differ in a few aspects from those applied by Kröger [5].

The mass flow rate and temperature distribution through the heat exchanger is assumed to be uniform. No heat transfer is modelled and the outlet air from the heat exchanger is assumed to be at the heat exchanger temperature. In the current study the upper surface of the heat exchanger is modelled as a source and the bottom surface as a sink. It is assumed that the pressure rise due to the fans is cancelled by the pressure drop over the heat exchanger. The values of the turbulence parameters at the top of the heat exchanger are based on an assumed turbulence intensity of 25%. The pressure boundary values shown are the "reduced pressure" values referred to earlier.

The velocities are all set to zero on the ground. The values of the velocities and the turbulence parameters near to the solid surface are calculated using the wall-functions described by Launder and Spalding [16].

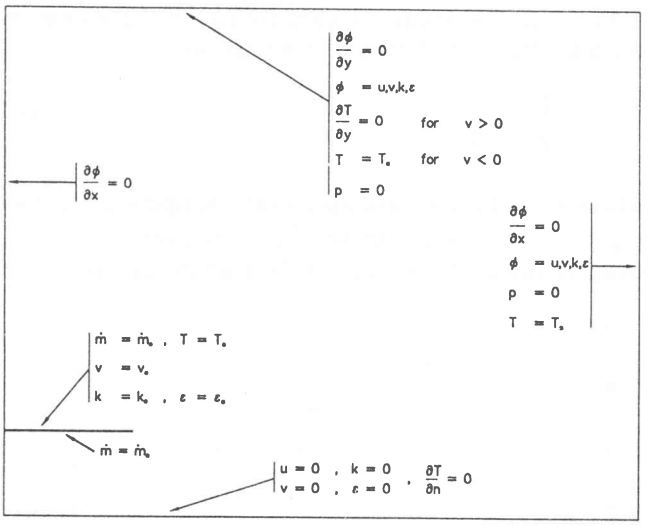

Fig. 2 Boundary conditions

At the upper atmospheric boundary a dual temperature boundary condition is applied. A zero gradient is prescribed at any point where outflow over the boundary occurs. When inflow over the boundary is encountered, the temperature is assumed to be equal to the ambient temperature.

Theoretical analysis

Consider the end of the heat exchanger at which recirculation occurs. For purposes of analysis, the heat exchanger and fan assembly is represented by a straight line at an elevation H above ground level as shown in Figure 3. Let the width of the heat exchanger be W. It is assumed that the air velocity entering the cooling tower along its periphery, V_i, is uniform and constant and in the horizontal direction. The outlet velocity, V_o, is similarly uniform and in the vertical direction.

Consider the particular streamline at the outlet of the heat exchanger that diverges from the plume and forms the outer "boundary" of the recirculating air stream. It is assumed that the distance, H_r, that it rises above the heat exchanger is the same as the distance H_r that it sinks below the heat exchanger. At the elevation $(H + H_r)$ it passes through a stagnation point and at the elevation $(H - H_r)$ the streamline enters the cooling tower at a velocity V_i. Let the highest position of the streamline be point 1 and the lowest position be point 2. By neglecting viscous effects, mixing, and heat transfer to the ambient air and applying Bernoulli's equation, we find for steady-state conditions:

$$p_1 + \rho_o g(H + H_r) = p_2 + \tfrac{1}{2}\rho_o V_i^2 + \rho_o g(H - H_r) \qquad (6)$$

It will be assumed that the total pressure at point 1 is constant and equal to the stagnation pressure of the ambient air, that is,

$$p_{a1} = p_1 \qquad (7)$$

Similarly, at point 2, the total pressure is given by

$$p_{a2} = p_2 + \tfrac{1}{2}\rho_a V_i^2 \qquad (8)$$

Substituting Eqs. (7) and (8) into Eq. (6), we find:

$$p_{a1} + \rho_o g H_r = p_{a2} - \tfrac{1}{2}\rho_a V_i^2 + \tfrac{1}{2}\rho_o V_i^2 - \rho_0 g H_r \qquad (9)$$

For the stagnant ambient air far from the tower,

$$p_{a1} - p_{a2} \approx \rho_a g H_r \qquad (10)$$

Substituting Eq. (10) into Eq. (9), we find:

$$H_r = \frac{V_i^2}{4g} \qquad (11)$$

According to the equation of mass conservation, the flow per unit depth of the tower can be expressed as:

$$\rho_o H_r V_i + \rho_a (H - H_r) V_i = \rho_o V_o W \qquad (12)$$

If the amount of recirculation is small, we obtain:

$$V_i \approx \frac{\rho_o V_o W}{\rho_a H} \qquad (13)$$

Lichtenstein [17] defines the recirculation factor r as

$$r = \frac{\dot{m}_r}{\dot{m}_a + \dot{m}_r} = \frac{\dot{m}_r}{\dot{m}} \qquad (14)$$

where $\dot{m}_r$ is the recirculating warm air mass flow rate, while $\dot{m}_a$ is the ambient air mass flow rate into the heat exchanger. Expanding Eq. (14), we obtain:

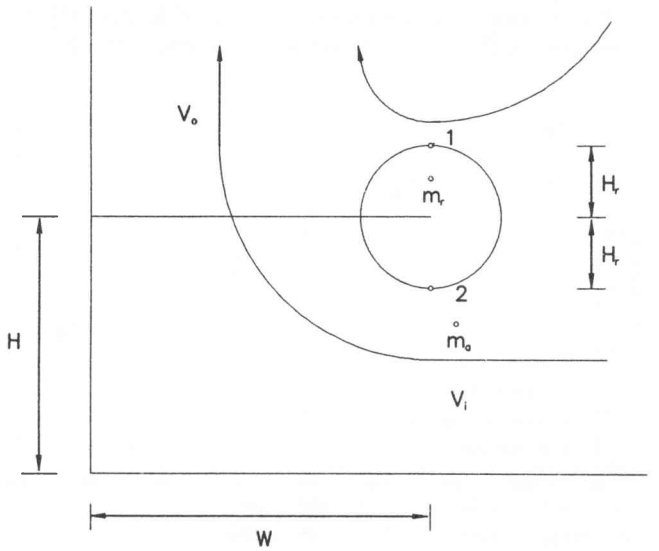

Fig. 3 Theoretical recirculation

$$r = \frac{\rho_o V_i H_r}{\rho_a V_i (H - H_r) + \rho_o V_i H_r}$$

$$\approx \frac{\rho_o H_r}{\rho_a H} \tag{15}$$

Substituting Eqs. (11) and (13) into Eq. (15), we find:

$$r = \frac{1}{4}\frac{V_o^2}{gW}\left(\frac{\rho_o W}{\rho_a H}\right)^3 \tag{16}$$

This is only half of the recirculation predicted by Kröger [5]. The effect of a wind wall or a deep plenum is to reduce the amount of recirculation taking place. If the height of the wind wall is taken as H_w, it can be shown (viz Kröger [5]) that the recirculation is given by:

$$r = \frac{1}{4}\left(\frac{\rho_o W}{\rho_a H}\right)^3 \frac{V_o^2}{gW}\left[1 - \frac{2(\rho_a - \rho_o g H_w}{\rho_o V_o^2}\right] \tag{17}$$

It is important to determine the effectiveness of the system when recirculation occurs. The effectiveness e_r of the heat exchanger is defined as

$$e_r = \frac{\text{heat transfer with recirculation}}{\text{heat transfer with no recirculation}} \tag{18}$$

The relationship between the recirculation and the effectiveness is complex in a real heat exchanger. Two extremes can, however, be evaluated analytically.

If it is assumed that the warm recirculating air does not mix at all with the cold ambient air, Kröger [5] shows that the effectiveness is given by:

$$e_r = 1 - r \tag{19}$$

If, however, it is assumed that the recirculating air mixes perfectly with the inflowing ambient air, Kröger [5] shows that the effectiveness is then given by:

$$e_r = \left(\frac{1-r}{T_o - T_a}\right) \left\{\frac{T_{he} - [T_{he} - (1-r)T_a]\exp(-UA/\dot{m}c_p)}{1 - r\exp(-UA/\dot{m}c_p)} - T_a\right\} \tag{20}$$

where T_{he} is the temperature of the heat exchanger, U the overall heat transfer coefficient, A the frontal area and c_p the specific heat coefficient. In this study the overall heat transfer coefficient is taken as $U = 2928 V_o^{0.5}$ W/m$^2 \cdot K$

Results

Two sets of results are discussed. The first set of results are for a geometry corresponding to a dimensionally similar version of the experimental unit described by Kröger [5]. The second set of results are for a geometry corresponding to that shown in Figure 2. The width of the heat exchanger is taken as $W = 70$ m and its height above ground level as $H = 45$ m.

In the current study the effectiveness of the system in the numerical simulation is evaluated as:

$$e_r = \frac{\bar{T}_o - \bar{T}_{ir}}{T_o - T_a} \tag{21}$$

where $\bar{T}_o$ is the mass averaged outlet temperature at the top of the heat exchanger and $\bar{T}_{ir}$ the mass averaged inlet temperature at the bottom of the heat exchanger.

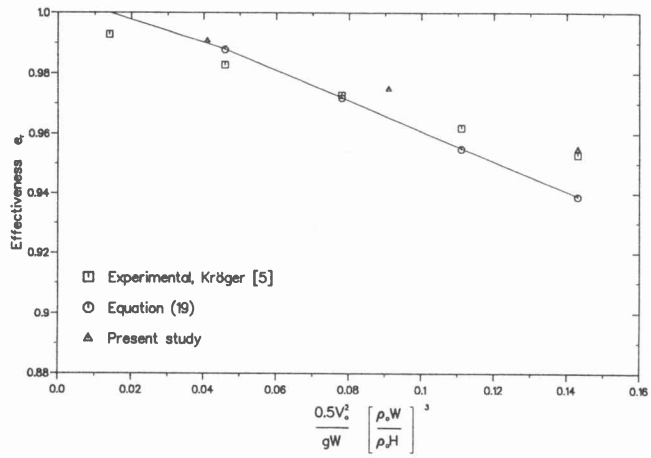

Fig. 4 Experimental heat exchanger effectiveness

The results of the calculation corresponding to the geometry of the experimental unit of Kröger [5] are compared graphically with the analytical solution for no mixing and the experimental data in Figure 4. The numerical results are in good agreement with the experimental data and the analytical solution. This seems to confirm the assumption that relatively little mixing takes place between the rising warm plume air and the incoming colder ambient air. The slight difference in slopes between the analytical solution and the numerical and experimental results might in part be due to the fact that the analytical theory does not take the exact geometrical configuration of the experimental heat exchanger into account.

In Figure 5 the analytical solutions for no mixing and perfect mixing, and the numerical data of Kröger [5] are compared with the corresponding numerical results for

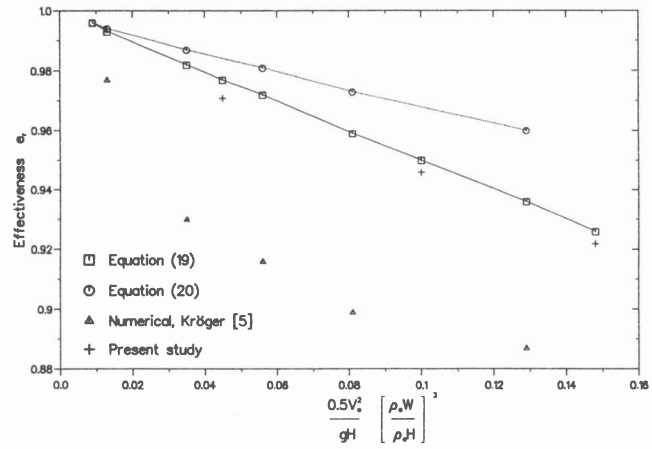

Fig. 5 Heat exchanger effectiveness

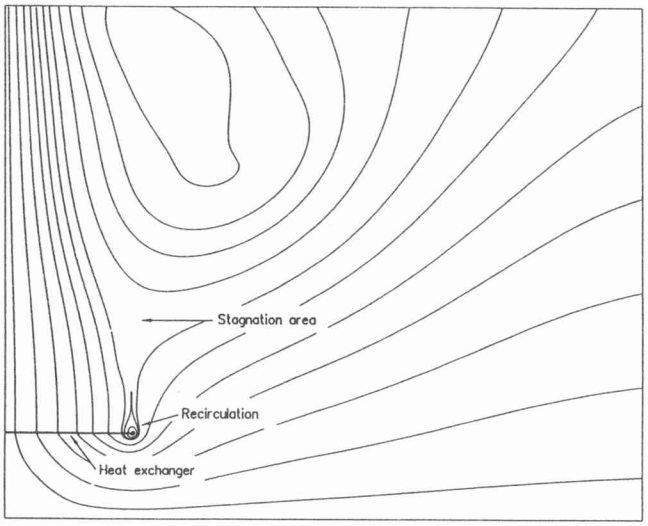

Fig. 6 Calcualated flow pattern

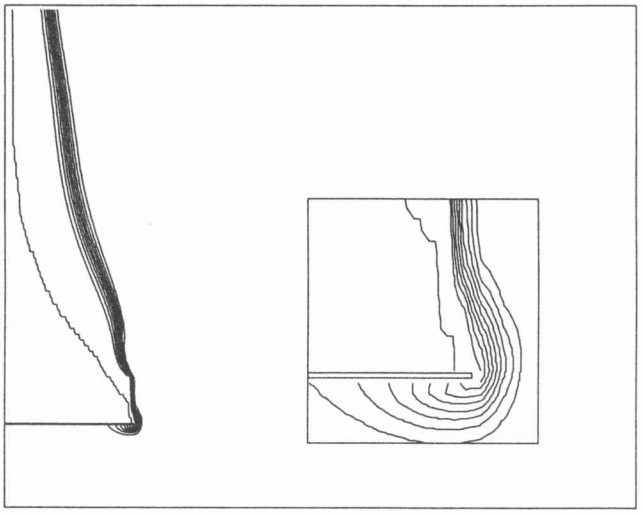

Fig. 7 Calculated temperature distribution

the second geometry. The current numerical results are in good agreement with the curve for no mixing. An Euler solution of the flow field has shown that there is only a small difference between the effectiveness for an inviscid solution and a viscid solution. This confirms that the flow process is dominated by gravitational forces and that very little mixing takes place. The fact that the numerical results exhibit the same trend as the analytical solutions is also an indication that the choice of dimensionless groups is a reasonable one. There is also a marked difference between the current numerical results and those of Kröger [5]. This is an indication that the boundary conditions applied by Kröger are probably deficient in certain respects.

A streamline plot of the flow field is shown in Figure 6. The streamlines are for an outlet velocity of $V_o = 8.5\ m/s$ and are calculated by following the velocity vectors through the flow field using the procedure outlined by Du Toit [18]. The streamlines show the presence of the large scale recirculating cell, as well as the recirculation at the end of the heat exchanger. The presence of a stagnation point between the two recirculating cells is also intimated. The flow field is in good agreement with the expected flow pattern. The corresponding temperature distribution is shown in Figure 7. The ambient air temperature is taken as $T_a = 293\ K$ and the outlet temperature at the top of the heat exchanger is taken as $T_o = 323\ K$. It can be seen that the warm air is confined to the bouyant plume and the recirculation zone at the end of the heat exchanger. This also confirms the assumption that very little mixing takes place between the warm air and the colder ambient air.

Although the current results are in better agreement, this still does not provide the final answer to the boundary condition question. Attention will have to be given to coupled far field and near field solutions via infinite boundary conditions or other means.

Conclusions

The effectiveness due to warm air recirculation of a mechanical-draught heat exchanger is determined numerically and analytically. The results are compared with experimental as well as with other numerical data.

The predicted flow field is in good agreement with the expected flow pattern and shows the various recirculating cells which are formed. The presence of a stagnation point between the recirculation cells above the heat exchanger is also observed.

The numerical results compare well with the experimental data and the analytical solution for no mixing. The results confirm the fact that the flow process is dominated by gravitational forces and that very little mixing takes place between the rising plume of warm air and the inflowing colder ambient air. However, attention will have to be paid to a more complete model of the heat exchanger, including amongst others heat transfer, before more definite conclusions can be drawn. The possibility of coupled far field and near field solutions must also be investigated to provide more appropriate boundary conditions for the inner solution.

Notwithstanding the shortcomings of the current numerical model, it can be said that the results illustrate the potential of numerical tools for the analysis of engineering problems which involves fluid flow and heat transfer. The analysis not only provides the engineer with the required information, but can also give the engineer valuable insight into the complex flow processes and improve his understanding of the problem.

References

1. J. F. Kennedy and H. Fordyce, Plume Recirculation and Interference in Mechanical Draft Cooling Towers, *Proc. Cooling Tower Environment Symp.*, University of Maryland, Baltimore, pp. 58-87, 1974.

2. P. R. Slawson and H. F. Sullivan, Model Studies on the Design and Arrangement of Forced Draft Cooling Towers to Minimize Recirculation and Interference. *Proc. Waste Heat Management and Utilization Conf.*, pp. 235-244, 1981.

3. A. Y. Gunter and K. V. Shipes, Hot air Recirculation by Air Coolers, *Chem. Eng. Prog.*, Vol. 68, pp. 49-58, 1972.

4. B. R. Becker, J. R. Stewart, T. M. Walter and C. S. Becker, A Numerical Model of Cooling Tower Plume Recirculation, *Mathl. Comput. Modelling*, Vol. 12, pp. 799-819, 1989.

5. D. G. Kröger, Reduction in Performance Due to Recirculation in Mechanical-Draft Cooling Towers, *Heat Transf. Engnrg.*, Vol. 10, pp. 37-43, 1989.

6. W. A. Schreüder, J. P. du Plessis and D. Sharma, Numerical Modeling of Atmospheric Boundaries, *Num. Heat Transf.*, Part B, Vol. 17, pp. 171-196, 1990.

7. W. A. Schreüder and J. P. du Plessis, Numerical Modeling of Interior Boundaries, *Num. Heat Transf.*, Part B., Vol. 17, pp. 197-215, 1990.

8. D. B. Spalding, A General Purpose Computer Program for Multi-Dimensional One and Two Phase Flow, *Mathematics and Computers in Simulation*. Vol 23, pp. 267-276, 1981.

9. D. B. Spalding, Mathematical Modeling of Fluid-Mechanics, Heat-Transfer and Chemical- Reaction Processes: A Lecture Course, HTS/80/1, Imperial College, London, 1980.

10. D. Radosavljevic and D. B. Spalding, Simultaneous Prediction of Internal and External Aerodynamic and Thermal Flow Fields of a Natural-Draft Cooling Tower in a Cross-Wind, *Proc. Int. Cooling Tower Conf.*, EPRI GS-6317, 1989.

11. W. Rodi, Turbulence Models and their Application in Hydraulics: A State of the Art Review, IAHR, 1980.

12. H. I. Rosten and D. B. Spalding, The PHOENICS Equations, TR/99, CHAM, Wimbledon, 1987.

13. H. I. Rosten and D. B. Spalding, The PHOENICS Beginner's Guide, TR/100, CHAM, Wimbledon, 1987.

14. H. I. Rosten and D. B. Spalding, The PHOENICS Reference Manual, TR/200, CHAM, Wimbledon, 1987.

15 S. V. Patankar, *Numerical Heat Transfer and Fluid Flow*, p. 88, New York, McGraw-Hill, 1980.

16. B. E. Launder and D. B. Spalding, The Numerical Computation of Turbulent Flows, *Comp. Meths. Appl. Mech. Engrg.*, Vol. 3, pp. 269-289, 1974.

17. J. Lichtenstein, Recirculation in Cooling Towers, *ASME Trans.*, pp. 1037-1042, 1951.

18. C. G. du Toit, Inverse Mapping in Finite Elements as Applied to the Calculation of Streamlines, *Proc. 9th Symp. Finite Element Meths. in South Africa*, 1989.